Solar Energy Materials & Solar Cells 101 (2012) 270–276

Contents lists available at SciVerse ScienceDirect

Solar Energy Materials & Solar Cells

journal homepage: www.elsevier.com/locate/solmat

Improving the damp-heat stability of copper indium gallium diselenide solar cells with a semicrystalline tin dioxide overlayer

B. Selin Tosun [a], Rebekah K. Feist [b], Aloysius Gunawan [a], K. Andre Mkhoyan [a], Stephen A. Campbell [c,*], Eray S. Aydil [a,**]

[a] Department of Chemical Engineering and Materials Science, University of Minnesota, 421 Washington Avenue SE, Minneapolis, MN 55455, United States
[b] Dow Solar Solutions, The Dow Chemical Company, 1381 Building, Office 201, Midland, MI 48667, United States
[c] Department of Electrical and Computer Engineering, 200 Union Street SE, Minneapolis, MN 55455, United States

ARTICLE INFO

Article history:
Received 18 August 2011
Received in revised form
3 January 2012
Accepted 10 February 2012
Available online 3 March 2012

Keywords:
CIGS
Damp heat stability
Tin dioxide

ABSTRACT

While copper indium gallium diselenide (CIGS) thin film solar cells with laboratory efficiencies exceeding 20% have been reported, these high efficiencies may degrade with time as the devices are exposed to humid environments. Specifically, it is well known that water can diffuse to the CIGS–CdS–ZnO heterojunction. This penetration must be reduced or stopped to increase the solar cell lifetime. Herein, we show that tin dioxide layers deposited on top of completed CIGS solar cells can significantly increase the device lifetime by forming a barrier against water diffusion. Specifically, in accelerated damp-heat tests, our best results showed that initially 8–12% efficient CIGS solar cells did not decay from this peak efficiency even after 240 h at 85 °C and 85% relative humidity. In comparison, under identical test conditions, the solar cells without the tin dioxide layer lost nearly 80% of their initial efficiency, within 24 h after commencing the test. We deposited the tin dioxide films by radio frequency magnetron sputtering from tin dioxide targets at 5 mTorr. Semicrystalline SnO_2 films deposited at room temperature had SnO_2 nanocrystals embedded in amorphous SnO_2 without grain boundaries. The semicrystalline films exhibited better damp-heat stability than crystalline films deposited at higher temperature. We infer from the slow open circuit voltage decay that water permeation to the p–n junction is reduced when semicrystalline SnO_2 overlayers are used to protect the solar cell. We attribute this difference in damp heat stability to the lack of grain boundary water diffusion in semicrystalline SnO_2 films.

1. Introduction

Copper indium gallium diselenide (CIGS) thin film solar cells have been commercialized during the last decade with accelerating growth in the recent years. Laboratory scale power conversion efficiency of CIGS solar cells is 20% [1], but the long-term stability still needs improvement. Typically, the long-term stability of solar cells is studied in accelerated damp-heat (DH) tests at 85 °C and 85% relative humidity (RH). It is now well established that the water penetration into the solar cell is the culprit because the dry heat tests do not cause any major changes in the cell performance while damp-heat tests degrade the solar cell dramatically [2,3]. Under damp-heat conditions, unprotected CIGS solar cell efficiencies degrade very rapidly to less than 50% of their initial efficiency [2,4–6]. This degradation is due to several factors including changes in the window and absorber layers as well as the corrosion of the metals [5–7]. The changes in window and absorber layers decrease both the open circuit voltage (V_{oc}) and the fill factor (*FF*), but do not affect the short circuit current density (J_{sc}) significantly [5–7]. The fill factor is thought to decrease because the resistance of the ZnO and/or the transparent conducting oxide layers (e.g., Al doped ZnO or Sn doped In_2O_3) increases [2,5,6,9–15]. The open circuit voltage is thought to decrease because the Fermi level in the CIGS near the CdS–CIGS interface increases [2,5,6,9–11,15].

The lifetimes of CIGS solar cell are increased by covering and encapsulating them in glass adding both weight and cost. Block copolymers such as ethyl vinyl acetate (EVA) may also be used but it is difficult to make organic encapsulants with comparable performance to inorganic glasses. Organic encapsulants may be more effective if changes in the solar cell can be made that decrease the burden on the encapsulant. Herein, we show that a thin tin dioxide (SnO_2) coating on the CIGS solar cell increases the solar cell lifetime in damp heat tests without an encapsulant layer. We believe that high resistance of SnO_2 to moisture

* Corresponding author. Tel.: +612 625 6608; fax: +612 625 5012.
** Corresponding author. Tel.: +612 625 8593; fax: +612 626 7246.
E-mail addresses: scampbell@umn.edu (S.A. Campbell), aydil@umn.edu (E.S. Aydil).

0927-0248/$ - see front matter © 2012 Elsevier B.V. All rights reserved.
doi:10.1016/j.solmat.2012.02.017

permeation retards the degradation of the solar cells. We report the evolution of SnO_2 over-coated CIGS solar cell power conversion efficiencies, *FF*, V_{oc}, and J_{sc} as a function of time in damp humidity tests and compare these results to those for uncoated CIGS solar cells.

2. Experimental

CIGS solar cells, [Fig. 1(a)], were fabricated on stainless steel foil by co-evaporation at 550 °C. The CIGS layer was approximately 2 μm thick. Following, 80 nm thick CdS was deposited on the CIGS film through chemical bath deposition. A 50 nm thick insulating layer of ZnO and a 150 nm thick tin doped indium oxide (ITO), were deposited on CdS by RF magnetron sputtering. Contact to the ITO was made with an evaporated Ni/Ag grid pattern that is connected to a thicker bus bar at the edge of the foil for electrical contact. The back contact was made with sputtered Mo on the stainless steel substrate and beneath the CIGS absorber layer. Transmission electron microscopy (TEM) analysis was conducted using an FEI Tecnai F-30 microscope with a Schottky field-emission electron gun operated at 300 keV [16].

Tin dioxide thin films with varying thickness were deposited on completed CIGS solar cells using RF magnetron sputtering. The film thickness was changed between 200 nm ± 20 nm and 500 nm ± 20 nm. The films were deposited at the RF power levels, 100 W, 150 W, and 250 W and at two different substrate temperatures, room temperature and 150 °C. For the films deposited at 150 °C, the substrates were kept at 150 °C for 10 min before starting the deposition. Prior to all depositions, the target surface was cleaned for 3 min by presputtering while a shutter protected the substrate. The base pressure in the sputtering chamber was 2×10^{-6} Torr and deposition sequence was started only after reaching this pressure or lower for each experiment. The sputtering pressure was kept constant at 5 mTorr, which was maintained by flowing 20 standard cm^3/min of sputtering gas (Ar) into the chamber. The sputtering guns were at 23.58° with respect to the substrate normal. The electronic and structural properties of SnO_2 films as a function of deposition conditions were published in a previous study [8].

The damp heat tests were conducted in a temperature and humidity controlled chamber at 85 °C and 85% relative humidity. The solar cells were taken out from the test chamber every 24 h and their current–voltage characteristics were measured. The control solar cells were tested under damp-heat conditions for

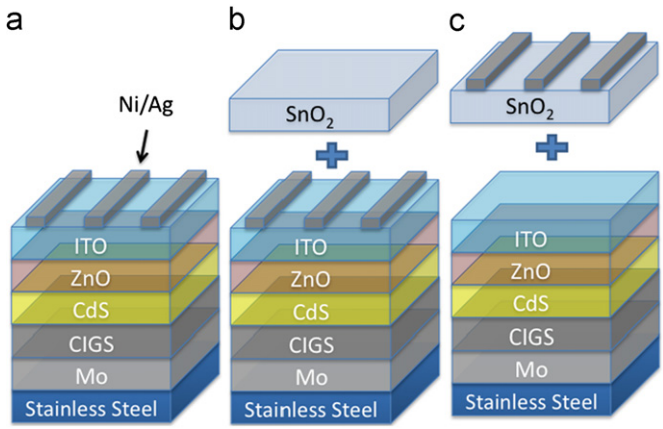

Fig. 1. (a) Conventional CIGS solar cell configuration. (b) CIGS solar cell configuration with SnO_2 coating above the top collection grid. (c) CIGS solar cell configuration with SnO_2 coating between the top collection grid and the window layer.

Table 1
SnO_2 deposition conditions for the second CIGS solar cells set.

Solar cell sample name	SnO_2 deposition conditions		
	RF power (W)	$T_{substate}$ (°C)	Thickness (nm)
1	150	Room temp.	200
2	150	Room temp.	200
3	250	Room temp.	500
4	150	Room temp.	500
5	100	Room temp.	500
6	250	150	200

168 h, while the SnO_2-film-coated cells were tested under identical conditions for 240 h. The current–voltage characteristics of the solar cells were recorded periodically, under 100 mW/cm^2 (AM 1.5) illumination generated by a solar simulator equipped with a Xe-arc lamp. The solar cell figures of merit, the fill factor (*FF*), the open circuit voltage (V_{oc}), the short circuit current density (J_{sc}), and the cell efficiency ($\eta = FF\times J_{sc}\times V_{oc}$) were measured outside the damp-heat test chamber under ambient conditions (~25 °C). The shunt (R_{sh}) and the series (R_{sr}) resistances of the cells were also determined as a function of the damp-heat test exposure time.

Two types of tests were conducted. In one set of the experiments, SnO_2 films were deposited on complete CIGS solar cells over the metal current collecting grid as shown in Fig. 1(b). This set of solar cells was used to screen the most suitable SnO_2 sputtering conditions for improving stability. In the second set of experiments, SnO_2 films were deposited on the ITO layer beneath the metal collection electrodes as shown in Fig. 1(c). The deposition conditions of the SnO_2 thin films for these solar cells are given in Table 1. In this second set, the SnO_2 deposition conditions were chosen from those that yielded promising results in the first set of experiments. Unlike in other studies, no encapsulation was used [6]. Identical CIGS solar cells without the SnO_2 layer were used as the control samples and exposed to the same damp-heat testing for comparison. These cells are referred as the control solar cells in this article.

3. Results and discussion

Fig. 2 shows the results from the first set of experiments where the SnO_2 films were deposited on completed solar cells [Fig. 1(b)]. The SnO_2 films were deposited under twelve different sputtering conditions. Fig. 2(a) shows the efficiency of the solar cells, normalized to their initial efficiency, after 144 h and 216 h of damp-heat testing. Fig. 2(b) shows the absolute values of the efficiencies after 144 h and 216 h in the damp-heat testing chamber. The results are also compared with the unprotected CIGS solar cells, named as "Control" in the Fig. 2(a) and (b). To see if there is a trend with respect to the SnO_2 film properties and deposition conditions, we rank ordered the data in Fig. 2(a) in decreasing performance after 216 h. Firstly, it is obvious that SnO_2 films help increase the damp-heat durability of the CIGS solar cells because significant fraction of the SnO_2-coated cells performed better than the control sample after 216 h in the damp-heat test chamber. Secondly, the solar cells coated with SnO_2 films sputtered at room temperature show better durability than the solar cells coated with SnO_2 sputtered at 150 °C. For example, the top three films in Fig. 2(a) are all deposited at room temperature and retain approximately 70% of their initial efficiency as compared to the control solar cell whose efficiency has decayed to 30% of the initial value. The solar cell coated with 200 nm thick SnO_2 film deposited using 150 W RF plasma power at room

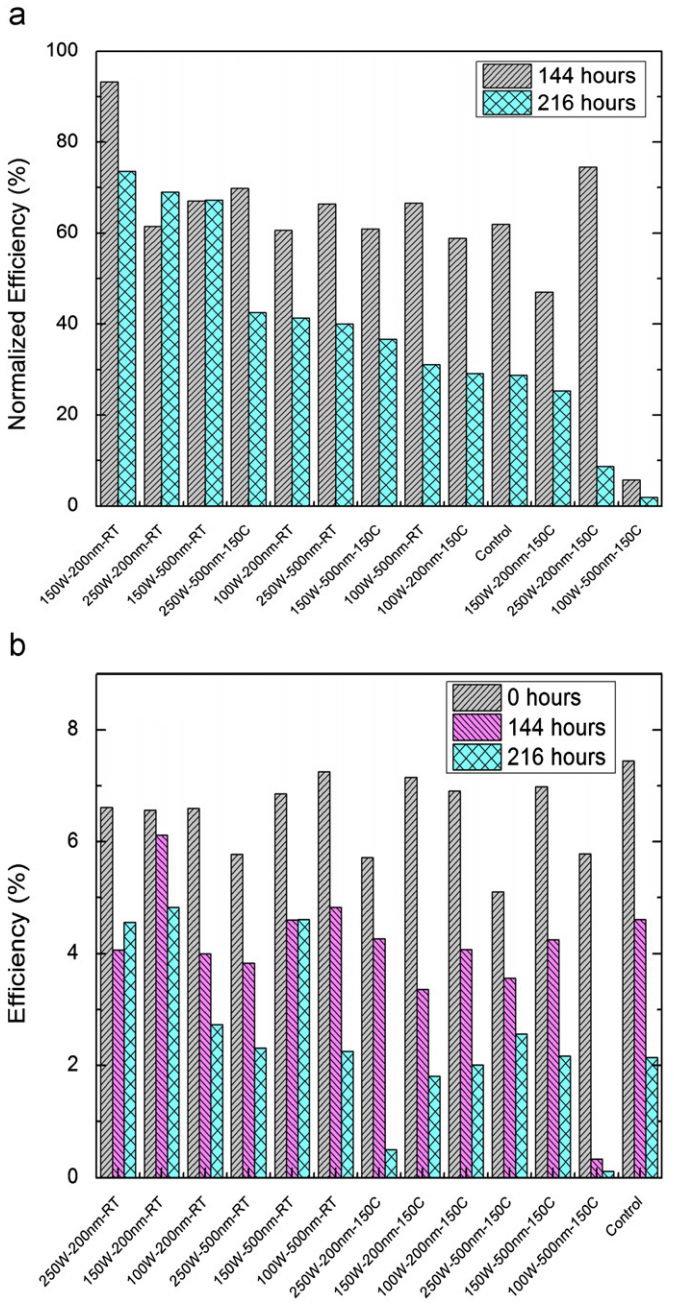

Fig. 2. (a) Solar cell stability performance for the solar cell configuration shown in Fig. 1(b). The efficiencies are normalized with respect to the initial solar cell efficiencies and ranked from left to right based on their performance after 216 h in the damp heat test chamber. (b) The absolute values of the solar cell efficiencies for the solar cells in (a).

temperature showed the best reliability. The SnO_2 films deposited at room temperature were a mixture of amorphous SnO_2 and nanocrystalline SnO_2 with nanometer size grains embedded in an amorphous matrix (semicrystalline) [8]. For example, Fig. 3 shows low- and high- resolution TEMs of SnO_2 films deposited under the same conditions, at room temperature using sputtering power of 150 W. Here we used a SiO_2-covered Si substrate for deposition of SnO_2. Semicrystalline nature of the SnO_2 film is apparent. The TEM images show nanocrystalline SnO_2 embedded in amorphous SnO_2. In these films there are no grain boundaries to facilitate water diffusion. Based on the sizes of the crystalline grains and the thickness of the electron transparent sample, we estimated

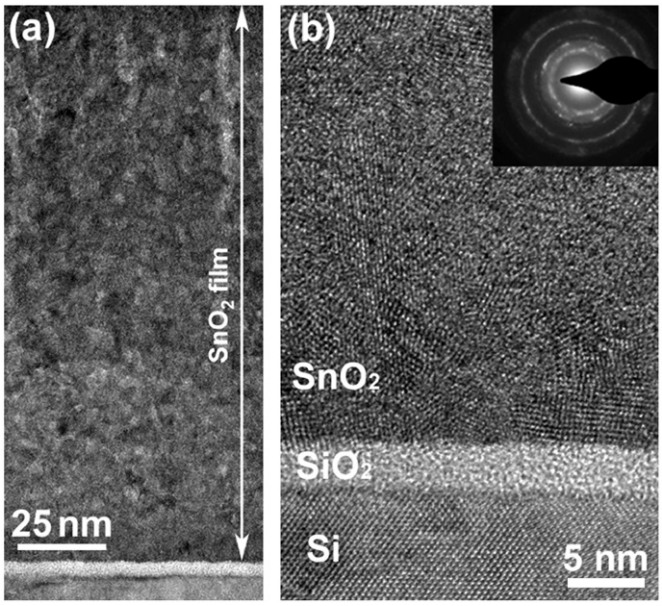

Fig. 3. (a) Low magnification and (b) high magnification TEM images of SnO_2 films deposited on SiO_2-coated Si substrate at room temperature using 150 W RF power. The inset is the diffraction pattern from the SnO_2 film confirming the semicrystalline structure of the film.

that the fraction of the crystalline grains is 25–30% of the total film. In contrast, films deposited at 150 °C tended to be more crystalline with grains abutted against each other [8]. The better protection performance of the semicrystalline films compared to polycrystalline films is attributed to the lack of grains and therefore lack of the grain boundary diffusion of water. The fraction of crystalline grains was calculated by estimating the average grain size and number of grains from TEM images, including one presented in Fig. 3. From low-loss EELS data the thicknesses of the sample was measured to be ~60 nm [17,18]. The volume fraction of the crystalline grains was then computed to be 25–30%, which also takes into account that depending on location of the grain within a specimen some of the grains will not be visible [19].

Fig. 4 shows the changes in the power conversion efficiency, fill factor, open circuit voltage, and short circuit current density as well as the changes in the shunt and series resistances as a function of damp-heat test time for the unprotected control solar cells. Each substrate had eight solar cells. The results in Fig. 4 are from those cells on each substrate, which showed the best performance under damp heat test conditions. The power conversion efficiencies of the unprotected solar cells decreased rapidly from 8–12% to less than 3% within 48 h as a function of damp-heat test time. Similarly, the fill factor for these control cells decreased within 48 h from ~70% to ~25% [Fig. 4(b)]. Fig. 4(c) shows the evolution of the open circuit voltage of these control solar cells as a function of damp-heat test time. The open circuit voltage dropped by approximately 50% from ~0.65 V in the first 24–48 h and then decayed more slowly to ~0.12 V. Fig. 4(d) shows that the short circuit current density, J_{sc}, only lost 10% of its initial value, a noticeable but otherwise insignificant decrease when compared to other solar cell figures of merit. Fig. 4(e) and (f) show the evolution of the series and the shunt resistances, respectively, as a function of damp-heat test time. The series resistance increased from ~5 Ω to 10–30 Ω within the first 48 h but eventually saturated at approximately $10 \pm 2\ \Omega$ after 168 h of DH exposure. The series resistances in CIGS solar cells is higher than crystalline silicon solar cells, because it contains multiple junctions and layers (e.g., transparent

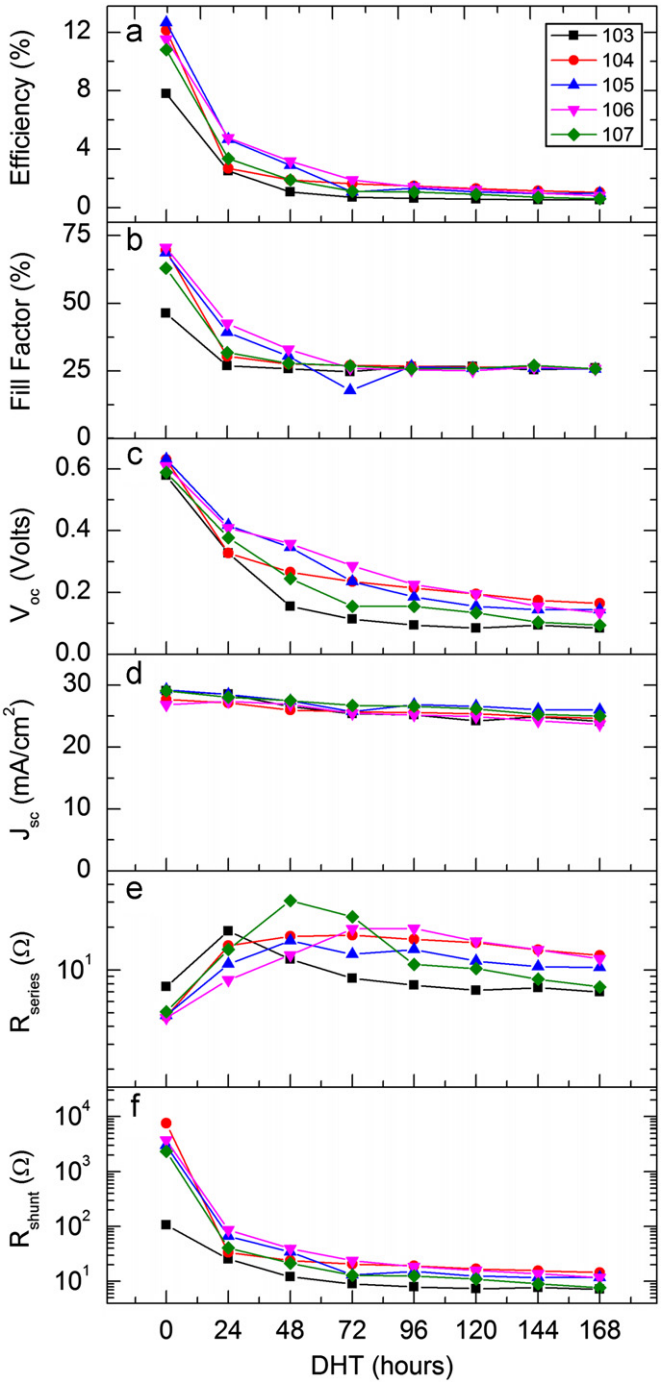

Fig. 4. (a) Efficiency (η), (b) fill factor (FF), (c) open circuit voltage (V_{oc}), (d) short circuit current density (J_{sc}), (e) series resistance (R_{sr}), and (f) shunt resistance (R_{sh}) of the control solar cells as a function of damp-heat exposure time (DHT).

conducting oxide) each with higher sheet resistances compared to crystalline silicon solar cells. More dramatic changes in the shunt resistance were observed. The shunt resistance decreased exponentially with damp-heat test time by three orders of magnitude during the first 72 h and saturated after reaching approximately 5–20 Ω. Fig. 5 shows the evolution of the current–voltage (J–V) characteristics of a typical control solar cell. The fill factor decreases without a significant drop in the J_{sc} and the J–V characteristic degrades by pivoting around (0, J_{sc}) point. This shows that the dramatic drop in the shunt resistance is responsible for the decrease in the fill factor and the effect of the changing series resistance is small in comparison.

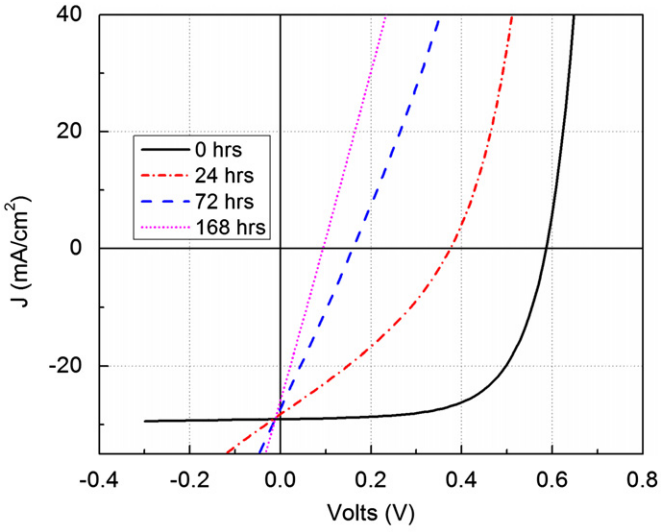

Fig. 5. Temporal evolution of the current–voltage characteristic of an uncoated control CIGS solar cell as a function of damp heat exposure time.

The observations in Fig. 4 on the degradation of control solar cells are consistent with the previously published reports. The increase in series resistance is attributed to the increase in ZnO and ITO resistivities [2,5,6,9–15]. The penetration of water to the CIGS absorber layer is believed to decrease the carrier concentration in the CIGS layer and to increase the Fermi level in the p-type absorber, E_{FP}, [2,5,6,9–11,15]. The increase in E_{FP} explains the decrease in open circuit voltage. In addition, the carrier concentration in the ZnO layer may also be decreasing which lowers the Fermi level, E_{FN}, in the n-type ZnO and therefore the open circuit voltage [5,12,13]. Decrease in carrier concentration and carrier mobility has also been observed in ITO films [14]. Lower carrier concentration in CIGS can also increase series resistance of the solar cell and contribute to the decrease in the fill factor [2,5,6,9–11,15]. Shunt resistance decrease with damp heat exposure has been observed previously [5,10] though there are only a few reports and the reasons are not well understood. Igalson et al. [5] attributed the shunt resistance decrease to changes in the grain boundaries of the absorber. One possibility is that water permeation alters the CIGS grain boundaries forming high conductance paths in the absorber, though the nature of these conductive pathways remains unclear. A second possibility is that the damp heat treatment increases the leakage across the ZnO–CdS–CIGS interface through the emergence of trap-assisted tunneling as a current leakage mechanism after damp heat treatment [5].

Fig. 6 shows the evolution of η, FF, V_{oc}, J_{sc}, R_{sh}, and R_{sr} as a function of damp-heat test time for SnO_2-coated solar cells [Fig. 1(c)]. The deposition conditions for the SnO_2 film used for each solar cell are listed in Table 1. Each substrate had eight solar cells. The results in Fig. 6 are from those cells, which showed the best performance under damp heat test conditions. Compared to Fig. 4(a), the power conversion efficiencies of the SnO_2-coated solar cells do not drop rapidly, and there is significant improvement in their damp-heat stability [Fig. 6(a)]. Some solar cells (e.g., 1, 2, and 4) maintain their initial power conversion efficiency even after 240 h under damp-heat conditions while other cells (e.g., 3, 5, and 6), though still better than the control solar cells, show 15–50% drop from their initial efficiencies. Among the solar cells that show 15–50% drop, the degradation rate is not uniform in time. For example, in some solar cells (e.g., 5) the initial power conversion efficiency was maintained for the first 4 days but degradation accelerated thereafter. Fig. 6(c) shows the evolution

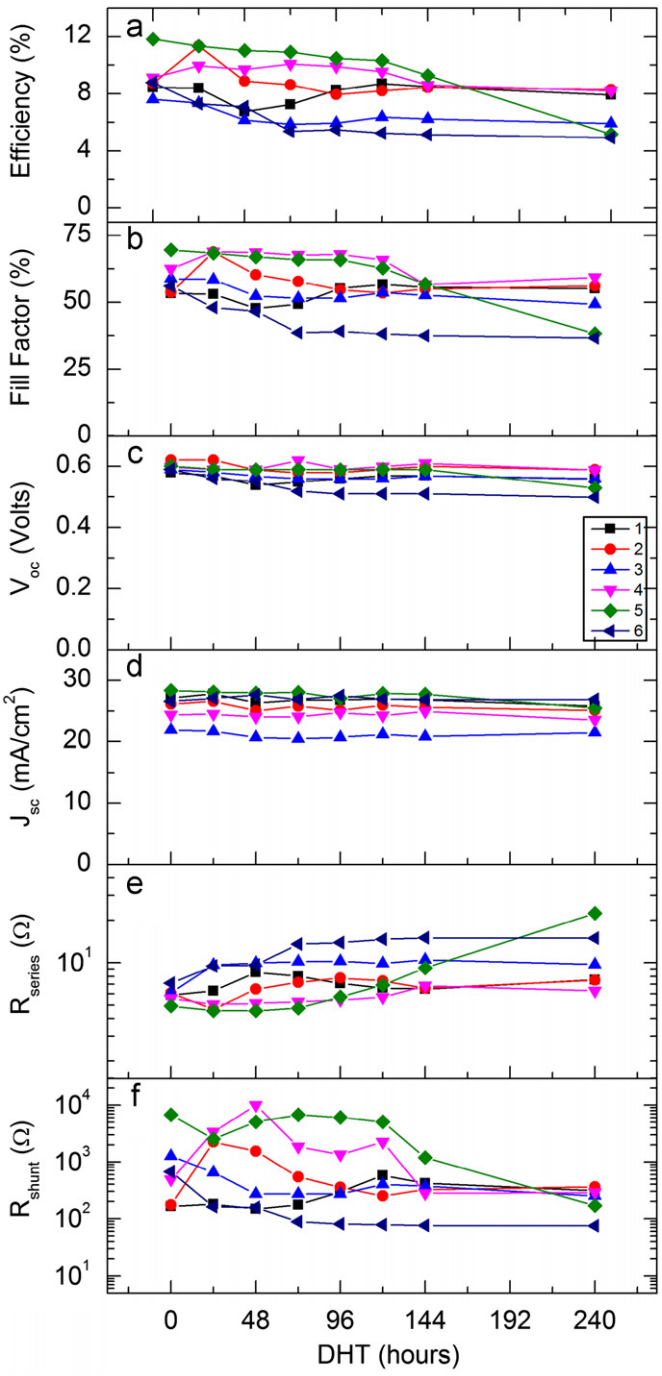

Fig. 6. (a) Efficiency (η), (b) fill factor (FF), (c) open circuit voltage (V_{oc}), (d) short circuit current density (J_{sc}), (e) series resistance (R_{sr}), and (f) shunt resistance (R_{sh}) of SnO_2-coated solar cells as a function of damp-heat exposure time (DHT).

of the open circuit voltage as a function of damp-heat test time. The open circuit voltages of all cells decreased less than 8% from their initial values even after 240 h in the damp-heat test chamber. Since the open circuit voltage decay is typically attributed to change in the Fermi levels E_{FN} and E_{FP} in ZnO and CIGS, respectively, [2,5,6,9–15], we conclude that these levels and therefore the carrier concentrations in the ZnO and CIGS layers are not affected significantly by the damp-heat test conditions when the cells are coated with a thin layer of semicrystalline SnO_2. The insignificant change in the open circuit voltage suggests that the semicrystalline SnO_2 inhibits water penetration through the ZnO layer to the CdS and CIGS layers. The short circuit current density, shown in Fig. 6(d), also does not show any change even after 240 h of damp-heat testing. In solar cells where some degradation is observed (e.g., 3, 5, and 6), the decrease in the efficiency can be attributed almost solely to the decreasing

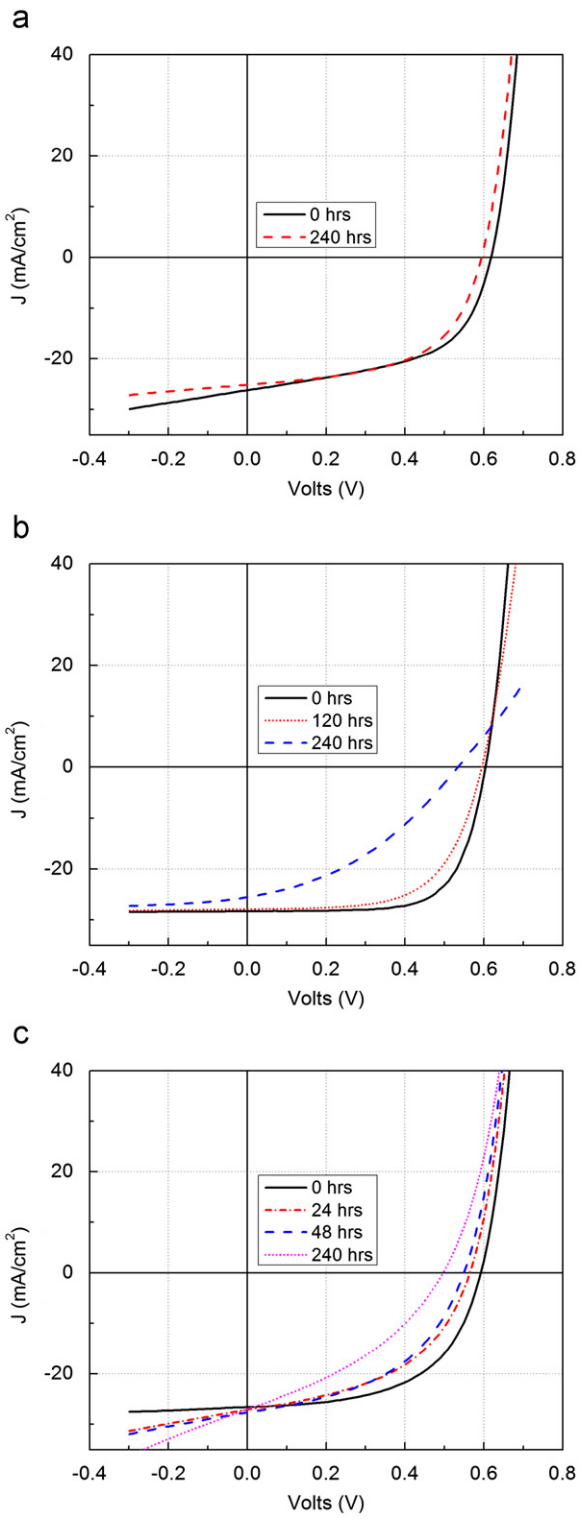

Fig. 7. Temporal evolution of the current–voltage characteristic of three representative SnO_2-coated [Fig. 1(c)] CIGS solar cells as a function of damp heat exposure time: (a) solar cell 2, (b) solar cell 5, and (c) solar cell 6. See Table 1 for SnO_2 deposition conditions and Fig. 6 for the temporal evolution of the solar cell figures of merit.

shunt resistance which in turn decreases the fill factor [Fig. 6(b)]. For example in solar cell 5 the efficiency, *FF*, R_{sr}, and R_{sh} remain constant for the first 4 days of the damp-heat test but after day 4, the shunt resistance decreases by two orders of magnitude coinciding with the drop in the *FF* and the efficiency. In contrast, the stable solar cells 1, 2, and 4 maintain their initial shunt and series resistances value for the entire duration (240 h) of the damp-heat stability test.

Fig. 7 shows the evolution of representative *J–V* characteristics from SnO_2-coated solar cells as a function of DH exposure time. Fig. 7(a) is the *J–V* characteristic of a solar cell coated with semicrystalline SnO_2 film deposited at room temperature (Cell 2 in Table 1 with corresponding TEMs shown in Fig. 3). After 240 h, except for a small decrease in V_{oc}, the *J–V* characteristic has not changed significantly compared to the *J–V* characteristic recorded prior to the damp heat test. In fact, the shunt resistance has improved. Fig. 7(b) shows the *J–V* characteristics for solar cell 5; this cell did not show degradation for approximately 4 days under DH conditions but degraded rapidly after day 4. Fig. 7(b) shows that, except for a slight increase in the series resistance, the *J–V* characteristic of this solar cell was unchanged after 120 h. However, after 240 h in DH conditions the series resistance had increased by a factor of four from $\sim 5\ \Omega$ to over $20\ \Omega$, while the shunt resistance had decreased by nearly two orders of magnitude from $\sim 6 \times 10^3\ \Omega$ to less than $\sim 200\ \Omega$. Nearly all of this degradation occurred after 120 h which is responsible for the decrease in the *FF* and the overall efficiency. The delayed decrease in the shunt resistance in the case of solar cell 5 can be an indicator of the delayed water penetration through the SnO_2 layer to the layers below. Finally, Fig. 7(c) shows the *J–V* characteristic of solar cell 6. The SnO_2 coating on this cell is fundamentally different in structure than the others, because it is deposited while maintaining the substrate at 150 °C. The films deposited at this temperature have much higher crystallinity and resemble polycrystalline films with grain boundaries rather that the semicrystalline structure in Fig. 3 [8]. As a consequence the films deposited at 150 °C is more prone to grain boundary water diffusion. Indeed, solar cell 6 is the worst performer of all cells. While slower, its *J–V* characteristic evolves in the same way the unprotected solar cells evolve (e.g., Fig. 5) as a function of damp heat exposure time.

4. Conclusions

We studied the ability of the RF magnetron sputtered SnO_2 films deposited on CIGS solar cells to protect the solar cells from humidity. Compared to uncoated control solar cells, the damp-heat durability of SnO_2-coated CIGS solar cells increased significantly. Specifically, the power conversion efficiency, the fill factor, and the open circuit voltage of the uncoated control solar cells decreased dramatically during damp-heat tests while their power conversion efficiencies dropped from ~12% to ~0.8% in 168 h. Consistent with previous reports, the decrease in the efficiency was caused by decreasing fill factor and open circuit voltage. The short circuit current density did not change significantly. In contrast, the solar cells protected with a SnO_2 overlayer deposited at room temperature maintained their initial power conversion efficiencies even after 240 h in the damp-heat test chamber at 85 °C and 85% relative humidity. In all SnO_2-coated solar cells, the short circuit current density and the open circuit voltage decreased less than 8% even after 240 h of damp-heat testing. Any observed decline in the power conversion efficiency is attributed mostly to the decreasing fill factor. The best damp-heat test protection was achieved with SnO_2 films sputtered at room temperature using 150 W RF power. Even a SnO_2 film as thin as 200 nm thick is adequate to improve the damp heat stability of CIGS solar cells. The semicrystalline structure of this SnO_2 layer, without grain boundaries, is believed to inhibit the moisture penetration. This structure eliminates diffusion of water molecules along the grain boundaries and provides a better protection from damp-heat conditions than polycrystalline films.

The tin dioxide layer is not an encapsulation. The tin dioxide layer is meant to decrease the water permeation requirements on thinner, flexible encapsulants by making the solar cell architecture more robust with respect to water permeation. That we do not observe degradation for 240 h under 85 °C and 85% even without an encapsulant is promising. Moreover, tin dioxide is a wide band gap material with high visible transmission [8] and high thermal and UV stability. Use of the tin dioxide layer in conjunction with flexible encapsulants is expected to help these encapsulants in exceeding module qualification according to IEC 61646 where the solar cells are expected to be stable for 1000 h under 85 °C and 85% relative humidity.

Acknowledgments

This work was funded by the Dow Chemical Company and by the Initiative for Renewable Energy and the Environment program of the University of Minnesota (IREE Grant M7-2008). This work utilized the University of Minnesota Characterization Facility, which receives partial support from the NSF-NNIN program and capital equipment funding from the NSF through the MRSEC program DMR-0819885. A.G. was funded through the MRSEC program DMR-0819885.

References

[1] I. Repins, M.A. Contreras, B. Egaas, C. DeHart, J. Scharf, C.L. Perkins, B. To, R. Noufi, 19.9%-efficient ZnO/CdS/CuInGaSe$_2$ solar cell with 81.2% fill factor, Progress in Photovoltaics 16 (2008) 235–239.
[2] J. Wennerberg, J. Kessler, L. Stolt, Cu(In,Ga)Se$_2$-based thin-film photovoltaic modules optimized for long-term performance, Solar Energy Materials and Solar Cells 75 (2003) 47–55.
[3] S. Spiering, D. Hariskos, S. Schonder, M. Powalla, Stability behavior of Cd-free Cu(In,Ga)Se$_2$ solar modules with In_2S_3 buffer layer prepared by atomic layer deposition, Thin Solid Films 480–481 (2005) 195–198.
[4] M. Powalla, B. Dimmler, Progress development of high performance CIGS modules for mass production, Thin Solid Films 387 (2001) 251–256.
[5] M. Igalson, M. Wimbor, J. Wennerberg, The change of electronic properties of CIGS devices induced by the damp heat treatment, Thin Solid Films 403–404 (2002) 320–324.
[6] C. Deibel, V. Dyakonov, J. Parisi, J. Palm, S. Zweigart, F. Karg, Influence of damp heat testing on the electrical characteristics of Cu(In,Ga)(S,Se)$_2$ solar cells, Thin Solid Films 403–404 (2002) 325–330.
[7] P.F. Carcia, R.S. McLean, S. Hegedus, Encapsulation of Cu(InGa)Se$_2$ solar cell with Al_2O_3 thin-film moisture barrier grown by atomic layer deposition, Solar Energy Materials and Solar Cells 94 (2010) 2375–2378.
[8] B.S. Tosun, R.K. Feist, S.A. Campbell, E.S. Aydil, Sputter deposition of semicrystalline tin dioxide films, Thin Solid Films 520 (2012) 2554–2561.
[9] J. Malmstrom, J. Wennerberg, L. Stolt, A study of the influence of the Ga content on the long-term stability of Cu(In,Ga)Se$_2$ thin film solar cells, Thin Solid Films 431–432 (2003) 436–442.
[10] M. Schmidt, D. Braunger, R. Schaffler, H.W. Schock, U. Rau, Influence of damp heat on the electrical properties of Cu(In,Ga)Se$_2$ solar cells, Thin Solid Films 361–362 (2000) 283–287.
[11] T. Yanagisawa, T. Kojima, T. Koyanagi, Behaviour of Cu(In,Ga)Se$_2$ solar cells under light/damp heat over time, Microelectronics Reliability 44 (2004) 229–235.
[12] J. Pern, R. Sundaramoorthy, C. Dehart, S. Glynn, X. Li, I. Repins, L. Mansfield, M. Contreras, R. Noufi, T. Gessert, N.R.E.L.C.I.G.S. Cell-Level Reliability Task and Studies. 〈http://www1.eere.energy.gov/solar/pdfs/pvrw2010_poster_pern.pdf〉, May 22nd 2011.
[13] W. Lin, R. Ma, J. Xuw, B. Kang, RF magnetron sputtered ZnO:Al thin films on glass substrates: a study zof damp heat stability on their optical and electrical properties, Solar Energy Materials and Solar Cells 91 (2007) 1902–1905.

[14] C. Guillen, J. Herrero, Stability of sputtered ITO thin films to the damp-heat test, Surface and Coatings Technology 201 (2006) 309–312.
[15] N.A. Allsop, A. Hansel, S. Visbeck, T.P. Niesen, M.C. Lux-Steiner, Ch.-H. Fischer, The dry and damp heat stability of chalcopyrite solar cells prepared with an indium sulphide buffer deposited by the spray-ILGAR technique, Thin Solid Films 511–512 (2006) 55–59.
[16] M.J. Behr, K.A. Mkhoyan, E.S. Aydil, Orientation and morphological evolution of catalyst nanoparticles during carbon nanotube growth, ACS Nano 4 (2010) 5087–5094.
[17] R.F. Egerton, Electron Energy-Loss Spectroscopy in the Electron Microscope, third edition, Springer, New York, 2011.
[18] K.A. Mkhoyan, T. Babinec, S.E. Maccagnano, E.J. Kirkland, J. Silcox, Separation of bulk and surface-losses in low-loss EELS measurements in STEM, Ultramicroscopy 107 (2007) 345–355.
[19] K.A. Mkhoyan, S.E. Maccagnano-Zacher, E.J. Kirkland, J. Silcox, Effects of amorphous layers on high-resolution ADF-STEM imaging, Ultramicroscopy 108 (2008) 791–803.